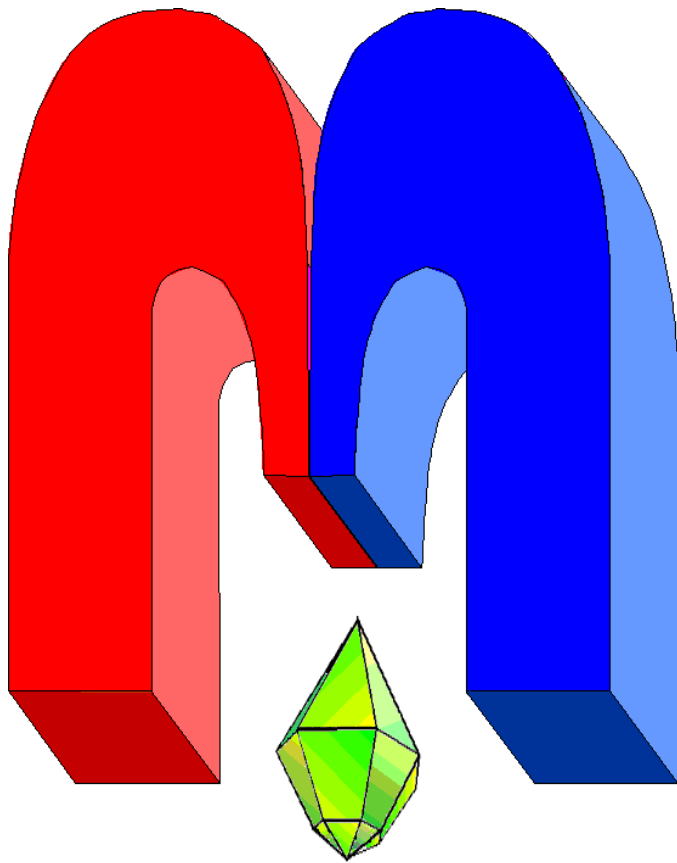


ISSN 2072-5981
doi: 10.26907/mrsej



***Magnetic
Resonance
in Solids***

Electronic Journal

Volume 25

Issue 3

Article No 23301

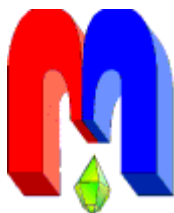
1-9 pages

2023

doi: [10.26907/mrsej-23301](https://doi.org/10.26907/mrsej-23301)

<http://mrsej.kpfu.ru>

<http://mrsej.ksu.ru>



Established and published by Kazan University*
Endorsed by International Society of Magnetic Resonance (ISMAR)
Registered by Russian Federation Committee on Press (#015140),
August 2, 1996
First Issue appeared on July 25, 1997

© Kazan Federal University (KFU)†

"Magnetic Resonance in Solids. Electronic Journal" (MRSej) is a peer-reviewed, all electronic journal, publishing articles which meet the highest standards of scientific quality in the field of basic research of a magnetic resonance in solids and related phenomena.

Indexed and abstracted by
Web of Science (ESCI, Clarivate Analytics, from 2015), Scopus (Elsevier, from 2012), RusIndexSC (eLibrary, from 2006), Google Scholar, DOAJ, ROAD, CyberLeninka (from 2006), SCImago Journal & Country Rank, etc.

Editor-in-Chief

Boris **Kochelaev** (KFU, Kazan)

Honorary Editors

Jean **Jeener** (Universite Libre de Bruxelles, Brussels)

Raymond **Orbach** (University of California, Riverside)

Executive Editor

Yurii **Proshin** (KFU, Kazan)
mrsej@kpfu.ru



This work is licensed under a [Creative Commons Attribution-ShareAlike 4.0 International License](https://creativecommons.org/licenses/by-sa/4.0/).



This is an open access journal which means that all content is freely available without charge to the user or his/her institution. This is in accordance with the [BOAI definition of open access](https://www.boai.ru/).

Technical Editor

Maxim **Avdeev** (KFU, Kazan)

Editors

Vadim **Atsarkin** (Institute of Radio Engineering and Electronics, Moscow)

Yurij **Bunkov** (CNRS, Grenoble)

Mikhail **Eremin** (KFU, Kazan)

David **Fushman** (University of Maryland, College Park)

Hugo **Keller** (University of Zürich, Zürich)

Yoshio **Kitaoka** (Osaka University, Osaka)

Boris **Malkin** (KFU, Kazan)

Alexander **Shengelaya** (Tbilisi State University, Tbilisi)

Jörg **Sichelschmidt** (Max Planck Institute for Chemical Physics of Solids, Dresden)

Haruhiko **Suzuki** (Kanazawa University, Kanazawa)

Murat **Tagirov** (KFU, Kazan)

Dmitrii **Tayurskii** (KFU, Kazan)

Valentine **Zhikharev** (KNRTU, Kazan)

* Address: "Magnetic Resonance in Solids. Electronic Journal", Kazan Federal University; Kremlevskaya str., 18; Kazan 420008, Russia

† In Kazan University the Electron Paramagnetic Resonance (EPR) was discovered by Zavoisky E.K. in 1944.

Magnetic properties of the double perovskite $\text{Sr}_2\text{CoNbO}_{6-\delta}$

D.V. Popov¹, R.G. Batulin², M.A. Cherosov², I.V. Yatsyk¹, T.I. Chupakhina³, Yu.A. Deeva³,
R.M. Eremina^{1*}, T. Maiti⁴

¹Zavoisky Physical-Technical Institute, Federal Research Center “Kazan Scientific Center of RAS”, Kazan 420029, Russia

²Kazan Federal University, Kazan 420008, Russia

³Institute of Solid State Chemistry of the RAS (UB), Ekaterinburg 620990, Russia

⁴Department of Materials Science and Engineering, Indian Institute of Technology, Kanpur 208016, India

*E-mail: REremina@yandex.ru

(Received November 16, 2023; revised December 7, 2023;
accepted December 7, 2023; published December 11, 2023)

Double perovskite $\text{Sr}_2\text{CoNbO}_{6-\delta}$ was obtained using a novel pyrolysis method involving nitrate-organic mixtures of the corresponding components and studied by means of XRF, magnetization-based, and EPR methods. The oxygen content equal to 5.4 was obtained from X-ray fluorescence analysis and magnetization data. The effective magnetic moment is $4.05 \mu\text{B}$ per cell, that corresponds to the theoretical values. The phase transition to an ordered state in the temperature range of $5 \div 300$ K was not detected. The antiferromagnetic nature of exchange interactions between the spins of cobalt ions is confirmed by the negative sign of the Curie-Weiss temperature $\Theta = -50$ K obtained via fitting the inverse magnetic susceptibility. An exchange-narrowed line from cobalt ions is observed in the EPR spectrum in the temperature range of $5 \div 80$ K. A sharp increase in the linewidth at 80 K is associated with the dynamic Jan-Teller effect.

PACS: 71.70.Ch, 75.10.Dg, 76.30.Kg, 71.70.Ej.

Keywords: double perovskite, magnetic resonance, EPR linewidth.

1. Introduction

The magnetic properties of double perovskites $\text{Sr}_2\text{MeNbO}_6$ (where Me = Cr, Mn, or Fe) have recently been actively studied in connection with their application as catalysts and thermoelectrics. The magnetic properties of double perovskites depend on the location of magnetic ions. As shown in [1, 2], two distinct Mn or Nb ions can form chains or planes. Quasi-one-dimensional properties are demonstrated in the temperature dependencies of magnetic susceptibility, magnetic-resonance linewidth, integrated EPR-line intensities, etc. However, the properties of $\text{Sr}_2\text{CoNbO}_6$ are still insufficiently described in the literature.

Cobalt-containing compounds are intriguing due to the ability of Co ions not only to have different valency, but also to exist in different spin states. Co^{3+} ions with a $3d^6$ electron configuration exhibit three distinct spin states: low-spin $S = 0$, intermediate-spin $S = 1$, and high-spin $S = 2$. Notably, the flexibility inherent in the spin states of Co^{3+} has stimulated interest in cobalts, particularly with regard to the spin-crossover phenomenon. This phenomenon involves an alternation in the spin state of an ion in response to external stimuli such as temperature, pressure, light irradiation, or an applied magnetic field. The Co_3BO_5 compound features simultaneous existence of high- and low-spin cobalt states [3]. Different-valence Co in structures with the same composition was demonstrated in LaSrCoO_4 [4].

The $\text{Sr}_2\text{CoNbO}_6$ compound ($\text{Sr}_{2-x}\text{La}_x\text{NbCoO}_6$ with $x = 0$) was studied in [5–7]. This compound has tetragonal phase with lattice parameters $a = b = 5.602 \text{ \AA}$ and $c = 7.921 \text{ \AA}$. The temperature dependencies of zero-field-cooling and field-cooling magnetization curves at

500 Oe exhibit separation at $T = 15$ K. The Curie-Weiss temperature was determined to be $\Theta_{CW} = -369$ K, and the effective magnetic moment was $4.60 \mu_B$, which corresponds to the theoretical effective magnetic moment of the compound with Co^{3+} ions only. A detailed analysis of the specific heat and AC susceptibility for magnetically frustrated $\text{Sr}_{2-x}\text{La}_x\text{CoNbO}_6$ ($x = 0$ to 1) double perovskites was carried out in [6].

Cobalt ions were doped into a non-magnetic compound $\text{Sr}_2\text{GaNbO}_6$. The features of the magnetic behavior of $\text{Sr}_2\text{Co}_{0.02}\text{Ga}_{0.98}\text{O}_6$ were presented in [8]. The synthesis of the $\text{Sr}_2\text{Co}_{0.02}\text{Ga}_{0.98}\text{NbO}_6$ compound was achieved through the flux method. X-ray diffraction analysis revealed a ceramic-type structure with a space group $I4/m$ and lattice parameters $a = 5.579(1) \text{ \AA}$ and $c = 7.902(1) \text{ \AA}$ [8]. The combination of spectroscopic studies supported by UV-vis-NIR absorption analysis unambiguously indicates an unusual mixed-spin state of Co^{3+} (with low- and intermediate-spin states) at room temperature in the $\text{Sr}_2\text{Co}_{0.02}\text{Ga}_{0.98}\text{NbO}_6$ double perovskite. An additional EPR measurement on this compound revealed EPR lines associated with cobalt ions in different spin states.

The properties of double perovskites differ significantly from the properties of their constituent parts. SrCoO_3 has space group $Pm3m$ with $a = 3.8289 \text{ \AA}$. It exhibits a ferromagnetic transition at $T = 305$ K and hysteresis loops, measured at $T = 2$ K in [9]. In contrast, $\text{SrCoO}_{2.5}$ has lattice parameters $a = 15.745 \text{ \AA}$, $b = 5.5739 \text{ \AA}$, and $c = 5.4697 \text{ \AA}$, and features an antiferromagnetic ordering below 537 K [10]. SrNbO_3 in a pseudocubic approximation has a lattice parameter $a = 4.023 \text{ \AA}$, although it was measured only as part of a thin film [11]. The objective of the present study is to investigate the magnetic properties of $\text{Sr}_2\text{CoNbO}_{6-\delta}$ using the EPR method and magnetometry.

2. Experimental details and results

The double perovskite $\text{Sr}_2\text{CoNbO}_{6-\delta}$ was synthesized using a novel pyrolysis method involving nitrate-organic mixtures of the corresponding components. Strontium nitrate ($\text{Sr}(\text{NO}_3)_2$), cobalt IV nitrate ($\text{Co}(\text{NO}_3)_2 \cdot 6\text{H}_2\text{O}$), and niobium oxide V (Nb_2O_5) served as starting reagents. Xylitol ($\text{C}_5\text{H}_7(\text{OH})_5$) was chosen as the organic component to facilitate the auto-ignition mode of the solution. This choice not only promotes the partial dissolution of niobium oxide in an alkaline solution but also acts as an organic fuel, enhancing the pyrolysis process of the reaction mass.

Stoichiometric amounts of cobalt and strontium nitrates were mixed with the corresponding amount of Nb_2O_5 . Distilled water and ammonium hydroxide (NH_4OH) were added to the mixture while controlling the pH of the solution ($\text{pH} = 12$), and the mixture was left for 24 hours. The reaction mixture was heated ($300 \div 350^\circ\text{C}$) until the solution ignited. The resulting nanodispersed powder was annealed at 950°C to eliminate carbon, followed by grinding and annealing at 1100°C for 8 hours.

X-ray examination was conducted using the Shimadzu XRD-7000 S automatic diffractometer with exposure time ranging from 3 to 5 seconds per point. The X-ray pattern processing was carried out using the FULLPROF-2018 software.

Based on X-ray diffraction data, the resulting compound was identified as a double perovskite $\text{Sr}_2\text{CoNbO}_{6-\delta}$ (Fig. 1). The structure of the double perovskite is visualized in Figure 2 using the DIAMOND 2 software.

The $\text{Sr}_2\text{CoNbO}_{6-\delta}$ phase is characterized by the tetragonal system with the space group $I/4m$ and lattice parameters $a = b = 5.65065(7) \text{ \AA}$ and $c = 7.97046(7) \text{ \AA}$.

X-ray phase analysis (XFA) conducted on a Bruker S2 Ranger X-ray fluorescence spectrometer

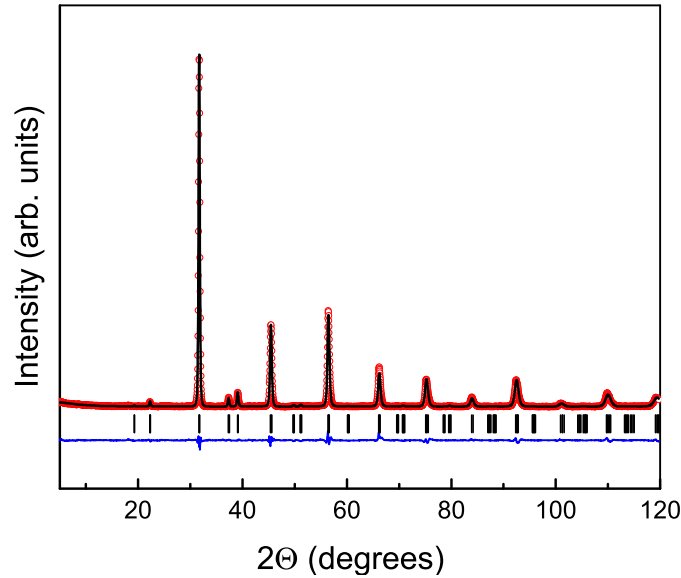


Figure 1. X-ray diffraction pattern of $\text{Sr}_2\text{CoNbO}_{6-\delta}$: experiment (red dots), its best fit (black line), their difference (blue line), and Bragg peaks (black dashes).

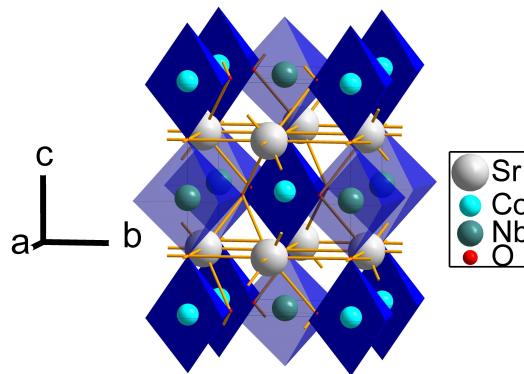


Figure 2. $\text{Sr}_2\text{CoNbO}_{6-\delta}$ structure: Sr ions (blue spheres), Co ions (cyan spheres), Nb ions (green spheres), and oxygen environments around Co and Nb ions (blue octahedra).

revealed an oxygen deficiency of $\delta \approx 0.8(3)$. Meanwhile, the concentrations of Nb and Co ions were found to be $0.99(5)$ and $0.95(5)$, respectively. Assuming the electrical neutrality in the sample, it can be inferred that the valence state of the cobalt ion is $2+$ rather than the anticipated $3+$.

Since Co ions exhibit a valence of $2+$ instead of the usual $3+$ for the double perovskite $\text{Sr}_2\text{CoNbO}_{6-\delta}$ and considering the relatively small margin of error in oxygen determination through X-ray fluorescence analysis, we recalculated the oxygen concentration to ensure the sample's electroneutrality. The recalculated oxygen concentration should be 5.4 instead of the expected 6 . This value closely aligns with the one obtained through the XRF analysis. Additionally, it was determined that the compound contains small amounts of impurities, including Cr (0.74%), Ni (0.24%), Ca (0.13%), Fe (0.05%), Ti (0.04%), and V (0.04%).

Temperature dependencies of magnetization were measured using the PPMS-9 device in both zero-field cooling (ZFC) and field cooling (FC) regimes within a temperature range of $5 \div 300$ K at an external magnetic field of 1 kOe. No local peaks or distinctions between ZFC and FC

curves were observed throughout the study. Additionally, no peaks were found in the first and second derivatives of the temperature dependence of magnetization.

The paramagnetic component of the inverse magnetic susceptibility was approximated using the Curie-Weiss law:

$$\chi = \frac{C}{T - \Theta_{CW}}, \quad (1)$$

where χ is the magnetic susceptibility, C is the Curie constant, T is the absolute temperature, and Θ_{CW} is the Curie-Weiss temperature [12]. The best Curie-Weiss-law fit is shown by the red line in Fig. 3. The fitting parameters are provided in Table 1.

The experimental and theoretical effective magnetic moments were calculated as:

$$\mu_{\text{eff}} = \sqrt{\frac{3kC}{N_A}}, \quad \mu_{\text{eff}}^{\text{Theor}} = g\sqrt{NS(S+1)}, \quad (2)$$

where N_A is the Avogadro constant, S is the spin moment of magnetic ions of number N , and g is the g -factor [12].

The theoretical effective magnetic moment was calculated assuming that Co²⁺ with $g = 2.1$ is the only magnetic ion in the compound. The calculation results are presented in Table 1. The theoretical moment is practically equal to the experimental one.

Table 1. The Curie constant, the Curie-Weiss temperature, and effective theoretical and experimental magnetic moments of Sr₂NbCoO_{6-δ}.

H (kOe)	Θ_{CW} (K)	C (K · emu/mol)	μ_{eff} (μ_B)	μ_{theor} (μ_B)
1	-50	2.05	4.05	4.06
10				

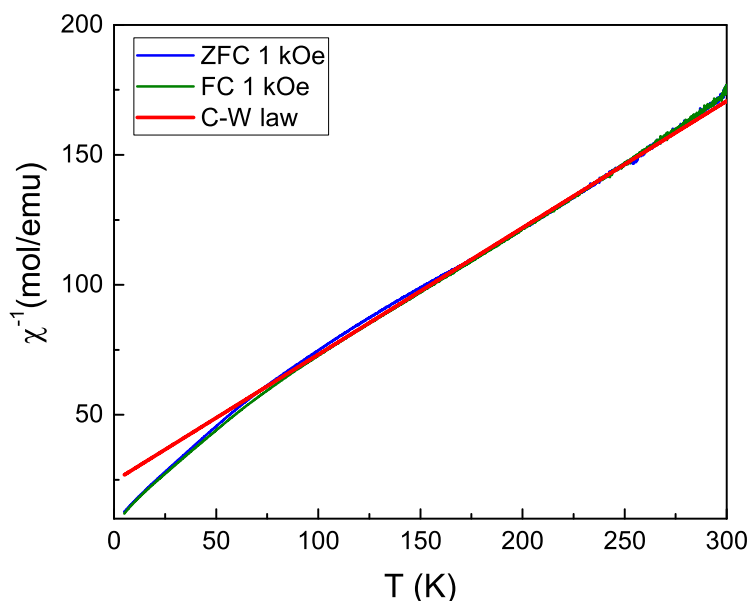


Figure 3. Temperature dependence of the inverse magnetic susceptibility (χ^{-1}) of Sr₂NbCoO_{6-δ} : experiments in ZFC (blue line) and FC (green line) regimes. Also shown by the red line is the best Curie-Weiss-law fit.

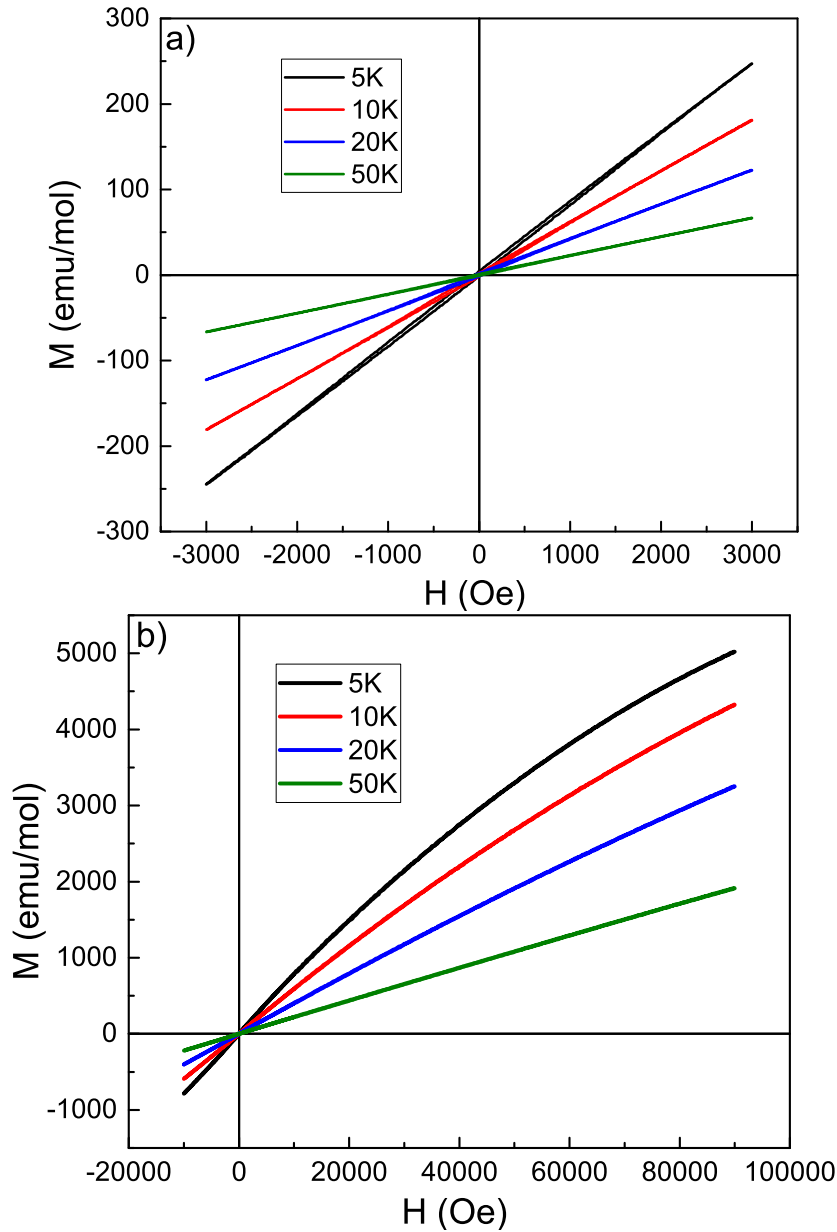


Figure 4. The dependence of magnetization on magnetic fields in $\text{Sr}_2\text{CoNbO}_{6-\delta}$, a) for external magnetic field values of ± 0.3 T, b) for external magnetic field values of ± 9 T,

Magnetic-field dependencies of magnetization were measured using the PPMS-9 device in the ± 0.3 T range of the external magnetic field at 5, 10, 20, and 50 K (Fig. 4a). Additionally, we carried out measurements with magnetic fields up to ± 9 T at the same temperatures (Fig. 4b). The magnetization isotherms demonstrate absence of hysteresis loops on the magnetic field, which indicates paramagnetic behavior in the $5 \div 300$ K range.

The ESR measurements were conducted at a frequency of ~ 9.4 GHz in the $5 \div 150$ K temperature range using the Bruker ELEXSYS E500-CW spectrometer equipped with a continuous-flow He cryostat. The spectra were fitted by two EPR lines with the following profile:

$$\frac{dP}{dH} = \frac{d}{dH} \left(\frac{\Delta H + \alpha(H - H_{\text{res}})}{(H - H_{\text{res}})^2 + \Delta H^2} + \frac{\Delta H - \alpha(H - H_{\text{res}})}{(H + H_{\text{res}})^2 + \Delta H^2} \right), \quad (3)$$

where H_{res} is the resonance-line position, ΔH is the resonance linewidth, and α is the asymmetry parameter [1]. The results of EPR measurements are shown in Fig. 5. The extracted temperature

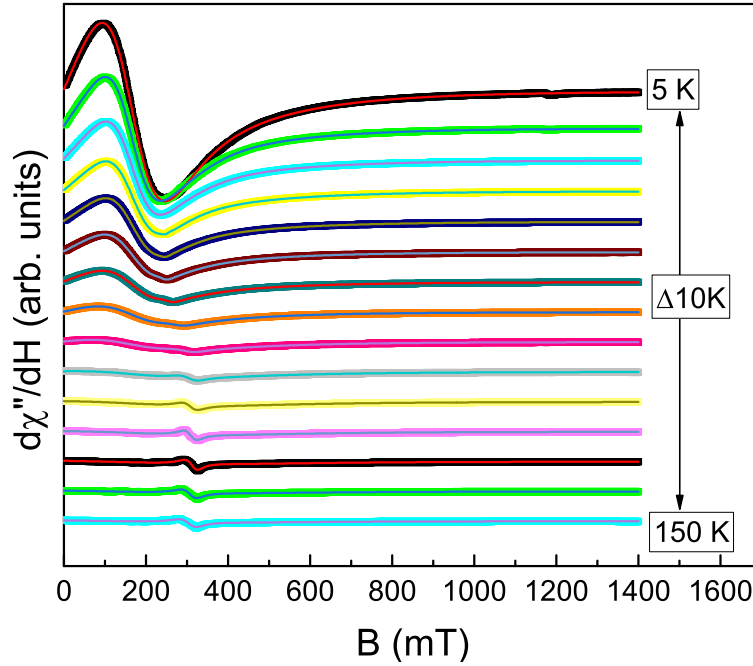


Figure 5. ESR lines of $\text{Sr}_2\text{CoNbO}_{6-\delta}$: experiments (thick lines) and their best fits (thin lines). Only every second line is shown.

dependencies of the parameters for each EPR line, including the linewidth ΔH , intensity I , and g -factor, are shown in Fig. 6.

The g -factor of the first EPR line is $g_{\text{eff}} = 4.2$ at 5 K and gradually increases to $g_{\text{eff}} = 6$ at 90 K. Most likely, this is due to the presence of splitting of Co^{2+} ion levels in ligand crystal field [13,14]. It is necessary to explain the ligand field energy level diagram of the ground state of high-spin Co^{2+} . Distortion splits the ground state into two Kramers doublets $m_s = \pm 1/2$ and $m_s = \pm 3/2$. If the corresponding energy splitting between the two doublets is positive, then $\pm 1/2$ has lower energies than $\pm 3/2$. We assume that we observe an EPR line between the $\pm 1/2$ states, then g_{eff} is defined as $g_{\text{eff}} = g \cdot \sqrt{S(S+1) - m_s(m_s - 1)}$. If $g = 2.1$, then $g_{\text{eff}} = 4.2$. This behavior is typical for Co^{2+} ions [16–18]. We believe that the intensity of the g -parallel component is much lower than the g -perpendicular one, which we denoted as g_{eff} . Such a component is present in the Q-band EPR spectrum Fig. 7.

The first EPR line with $g_{\text{eff}} \approx 4.2$ disappears at temperatures above 90 K. Such behavior is reminiscent of the EPR measurements for $\text{Sr}_2\text{Co}_{0.02}\text{Ga}_{0.98}\text{O}_6$, where a line at $g_{\text{eff}} = 4.27$ appears under certain temperatures [8]. To describe the experiment, the authors assumed that Co^{3+} in their compound is in different spin states. The value $g_{\text{eff}} \approx 4.2$ in our experiment is very different from the value of the effective g -factor obtained for Co^{3+} with $g = 2$ in LaCoO_3 [15]. The second EPR line has an intensity two orders of magnitude lower and is likely to appear due to impurities present in the sample, as indicated by the XRF analysis. This is further confirmed by the Q-band EPR measurements, in which multiple additional lines are clearly visible at high power levels of 5 and 10 dB (Fig. 7). We associate them with 3d impurity ions revealed via the XRF analysis, and g parallel component EPR spectra Co^{2+} .

For Co^{2+} ions, there occurs an electron-phonon interaction, also referred to as the dynamic Jahn-Teller (JT) interaction [19]. Therefore, the linewidth ΔH of the first EPR line was fitted

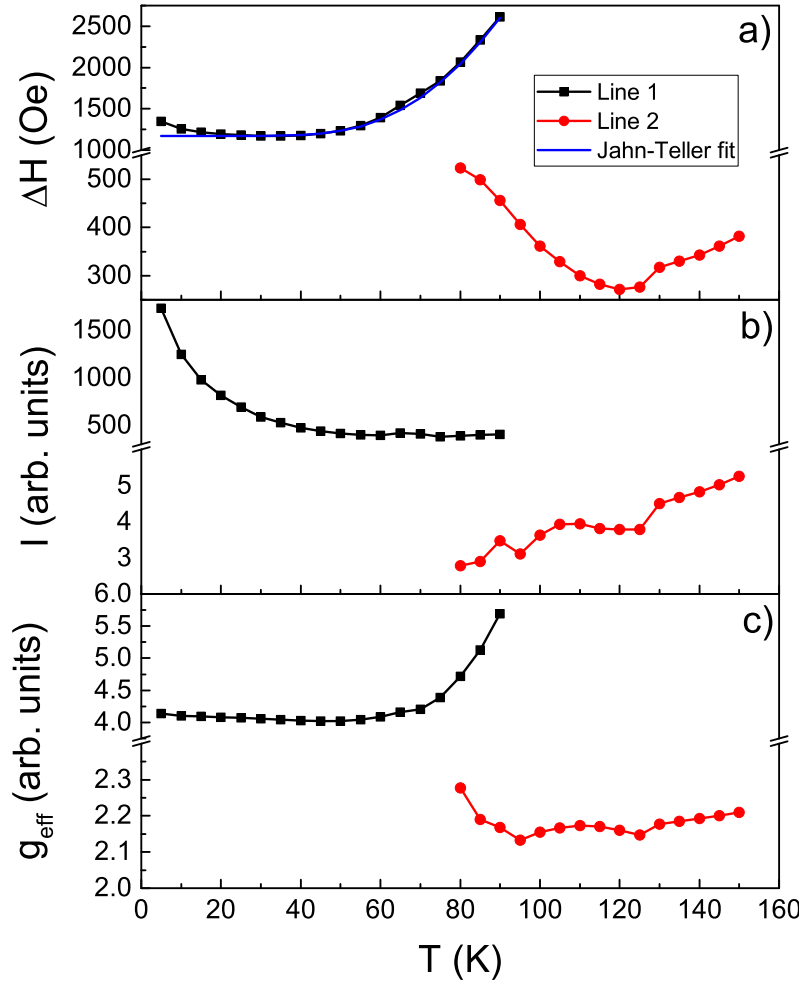


Figure 6. ESR-spectra fitting parameters of $\text{Sr}_2\text{CoNbO}_{6-\delta}$ for two EPR lines: (a) linewidth, (b) intensity, and (c) effective g -factor.

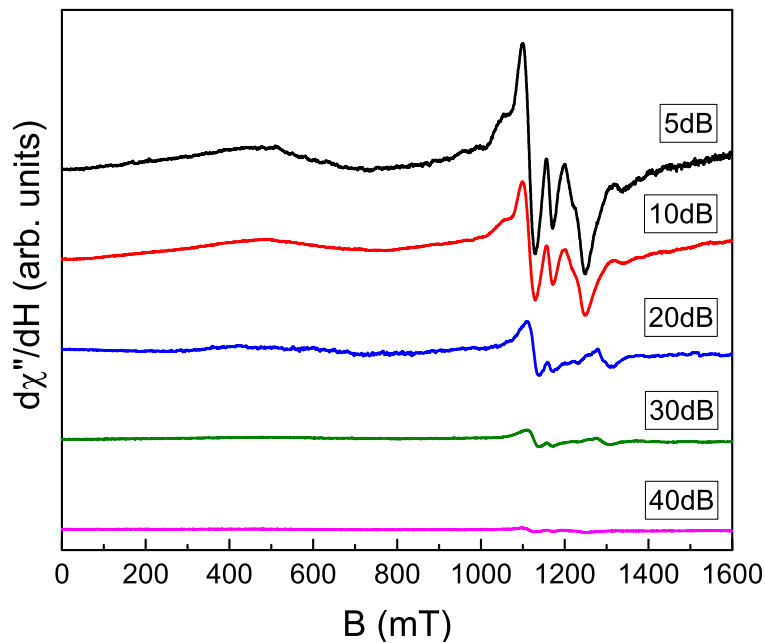


Figure 7. Q-band EPR spectra of $\text{Sr}_2\text{CoNbO}_{6-\delta}$ at $T=150$ K and at different microwave attenuations.

using the expression for Jahn-Teller ions:

$$\Delta H = \Delta H_0 + A \cdot \exp\left(-\frac{2\Delta}{T}\right), \quad (4)$$

where ΔH_0 is the residual linewidth, A is the prefactor, and Δ is the crystal-field splitting [20]. The fitting procedure suggested $\Delta H_0 = 1173$ Oe, $A = 74500$ Oe, and $\Delta = 178$ K. Similar value of $\Delta \approx 15$ meV was found in [21] as a result of excitonic Zeeman splitting in Co²⁺:ZnSe.

3. Conclusion

The double perovskite Sr₂CoNbO_{6-δ} was investigated through XRF, EPR, and magnetization measurements. Based on X-ray fluorescence analysis, we have determined that since the oxygen value is 5.4 instead of 6, the valence state of cobalt ions is 2+, as opposed to the expected 3+. No magnetic phase transitions were observed within the 5 ÷ 300 K temperature range. The Curie-Weiss temperature is negative ($\Theta_{CW} = -50$ K) and the theoretical effective magnetic moment is practically equal to the experimental one.

ESR spectra were analyzed as the sum of two EPR lines. The behavior of the first EPR line is characteristic of Co²⁺. The second EPR line is likely associated with impurities such as Cr, V, and Fe. Fitting the temperature dependence of the linewidth for the first EPR line revealed a crystal-field splitting value of $\Delta = 178$ K, which is consistent with the value of 15 meV observed in previous studies of Co²⁺: ZnSe [21].

Acknowledgments

This research was supported by the Russian Science Foundation (Project No. 22-42-02014) and DST Project number DST/INT/RUS/RSF/P-55/2021.

References

1. Popov D.V., Batulin R.G., Cherosov M.A., Yatsyk I.V., Chpakhina T.I., Deeva Yu.A., Eremina R.M. *JETP*, **37**(4), 643 (2023)
2. Popov D., Batulin R., Cherosov M., Vagizov F., Zinatullin A., Chupakhina T., Deeva Yu., Eremina R., Maiti T. *Magnetochemistry*, **9**(10), 219 (2023)
3. Kazak N.V., Platunov M.S., Knyazev Yu.V., Molokeev M.S., Gorev M.V., Ovchinnikov S.G., Pchelkina Z.V., Gapontsev V.V., Streltsov S.V., Bartolome J., Arauzo A., Yumashev V.V., Gavrilkin S.Yu., Wilhelm F., Rogalev A. *Phys. Rev. B*, **103**(9), 094445 (2021)
4. Yang N., Yu J., Zhang L., Sun Y., Zhang Y., Jiang B. *J. Water Process. Eng.*, **53**, 103804 (2023)
5. Kumar A., Dhaka R.S. *Phys. Rev. B*, **101**(9), 094434 (2020)
6. Kumar A., Schwarz B., Ehrenberg H., Dhaka R.S. *Phys. Rev. B*, **102**, 184414 (2020)
7. Kumar A., Shukla R., Kumar R., Choudhary R.J., Jha S.N., Dhaka R.S. *Phys. Rev. B*, **105**(24), 245155 (2022)
8. Varghese M., Simpson S., Lawrence G., Duttine M., Camacho P.S., Gaudon M., Toulemonde O. *J. Phys. Chem. C*, **126**, 8450-8460 (2022)
9. Long Y., Kaneko Y., Ishiwata S., Taguchi Y., Tokura Y. *J. Phys.: Condens. Matter*, **23**, 245601 (2011)

10. Munoz A., de la Calle C., Alonso J.A., Botta P.M., Pardo V., Baldomir D., Rivas J. *Phys. Rev. B*, **78**, 054404 (2008)
11. Oka D., Hirose Y., Nakao S., Fukumura T., Hasegawa T. *Phys. Rev. B*, **92**, 205102 (2015)
12. Kittel C. Introduction to Solid State Physics, 8th Edition, John Wiley & sons, inc, (2005). 704 pp.
13. Al'tshuler S. A. and Kozyrev B. M. Electron Spin Resonance: Electron Paramagnetic Resonance. Translated from the Russian edition (Moscow, 1961) by Scripta Technica. Charles P. Poole, Jr., Ed. Academic Press, New York, (1964). 372 pp.
14. Weckhuysen B.M., Verberckmoes A.A., Uytterhoeven M.G., Mabbs F.E., Collison D., de Boer E., Schoonheydt R.A. *J. Phys. Chem. B*, **104**(1), 37-42 (2000)
15. Ivanova S., Zhecheva E., Stoyanova R. *J. Phys. Chem. Solids*, **68**(2), 168-174 (2007)
16. Matsuda J., Kojima K., Yano H., Marusawa H. *J. Non-Cryst. Solids*, **111**(1), 63-66 (1989)
17. Sreedhar B., Sumalatha Ch., Yamada H., Kojima K. *J. Non-Cryst. Solids*, **203**, 172-175 (1996)
18. El-Malki E.M., Werst D., Doan P.E., Sachtler W.M. *J. Phys. Chem. B*, **104**(25), 5924-5931 (2000)
19. Wagner V., Koidl P. *J. Magn. Magn. Mater.* **15**, 33-34 (1980)
20. Heinrich M., Krug von Nidda H.-A., Krimmel A., Loidl A., Eremina R.M., Ineev A.D., Kochelaev B.I., Prokofiev A.V., Assmus W. *Phys. Rev. B*, **67**(22), 224418 (2003)
21. Norberg N.S., Parks G.L., Salley G.M., Gamelin D.R. *J. Am. Chem. Soc.*, **128**(40), 13195-13203 (2006)